JOURNAL OF SPACECRAFT AND ROCKETS
Vol. 44, No. 1, January–February 2007

Experimental Investigation of Solder Joint Defect Formation and Mitigation in Reduced-Gravity Environments

J. Kevin Watson*
NASA Johnson Space Center, Houston, Texas 77058
Peter M. Struk†
NASA John H. Glenn Research Center at Lewis Field, Cleveland, Ohio 44135
and
Richard D. Pettegrew‡ and Robert S. Downs§
National Center for Space Exploration Research, Cleveland, Ohio 44135

DOI: 10.2514/1.22842

This paper documents a research effort on reduced-gravity soldering of plated through-hole joints. Significant increases in joint porosity and changes in external geometry were observed in joints produced in reduced gravity as compared with normal gravity. Multiple techniques for mitigating the observed increase in porosity were tried, including several combinations of flux and solder application techniques, and demoisturizing the circuit board before soldering. Results were consistent with the hypothesis that the source of the porosity is a combination of both trapped moisture in the circuit board itself, as well as vaporized flux that is trapped in the molten solder. Other topics investigated include correlation of visual inspection results with joint porosity, pore size measurements, limited pressure effects (0.08–0.1 MPa) on the size and number of pores, and joint cooling rate.

Nomenclature

A = time-averaged magnitude of the three-dimensional acceleration
A_x = magnitude of acceleration in the longitudinal axis of the aircraft
A_y = magnitude of acceleration in the lateral axis of the aircraft
A_z = magnitude of acceleration in the vertical axis of the aircraft
C_P = specific heat of solder (60/40 wt% Sn/Pb), $173\ \mathrm{J/kg\cdot K}$
g = local gravitational acceleration
g_e = normal gravitational acceleration at sea level ($9.81\ \mathrm{m/s^2}$)
h_f = latent heat of solidification for solder (60/40 wt% Sn/Pb), $37{,}000\ \mathrm{J/kg}$
L = characteristic length scale for PTH solder joint
L_B = fillet leg length on the side of the joint opposite to which solder alloy was added (i.e., the "bottom")
L_T = fillet leg length on the side of the joint to which the solder alloy was added (i.e., the "top")
m = solder joint mass
Q = total thermal energy of solder joint, J
Q_{av} = average thermal energy transfer rate from the solder joint, W
T_P = measured peak solder temperature, K
T_M = solder (60/40 wt% Sn/Pb) melting temperature, 456 K
t = time, s
t_c = cooling time of solder joint from heating iron removal to solidification, s
ρ = molten solder density ($8500\ \mathrm{kg/m^3}$)
σ = surface tension of liquid solder ($0.481\ \mathrm{N/m}$)

Received 30 January 2006; revision received 27 April 2006; accepted for publication 7 May 2006. Copyright © 2006 by the American Institute of Aeronautics and Astronautics, Inc. The U.S. Government has a royalty-free license to exercise all rights under the copyright claimed herein for Governmental purposes. All other rights are reserved by the copyright owner. Copies of this paper may be made for personal or internal use, on condition that the copier pay the $10.00 per-copy fee to the Copyright Clearance Center, Inc., 222 Rosewood Drive, Danvers, MA 01923; include the code $10.00 in correspondence with the CCC.

*Aerospace Engineer, Exploration Office, Mail Code EX, 2101 NASA Road 1.
†Aerospace Engineer, Mail Code 110-3, 21000 Brookpark Road.
‡Associate Staff Scientist, Mail Code 110-3, 21000 Brookpark Road. Member AIAA.
§Student Researcher, Mail Code 110-3, 21000 Brookpark Road.

I. Introduction

WHETHER used occasionally for contingency repair or routinely in nominal repair operations, soldering will become increasingly important to the success of future long-duration human space missions. As a result, it will be critical to have a thorough understanding of the service characteristics of solder joints produced in reduced-gravity environments.

A limited amount of soldering has been performed onboard the Soviet/Russian Mir space station and, more recently, onboard the International Space Station (ISS) for contingency repairs. Whereas no reports have been made of operational failure of such repaired joints, no formal testing (either destructive or nondestructive) has been performed to characterize the changes that a reduced-gravity environment could have on such joints.

To date, a limited amount of experimental work has been conducted to assess the soldering process in reduced-gravity environments. Gap filling and microstructure have been investigated on sounding rocket flights [1]. Test results showed that wider annular gaps between concentric copper tubes could be filled with solder in low gravity via capillary action compared with normal-gravity conditions. In normal gravity, the molten solder alloy tended to accumulate in the lower portion of the annulus. An observed increase in the Cu-Sn η phase was attributed to slightly discrepant thermal cycles rather than to gravitational influences. Several Get Away Special payloads were flown on the Shuttle between 1982 and 1984 [2]. Although the success of these efforts was mixed, they demonstrated the influence of surface tension on the soldering process. Additionally, the potential for flux entrapment in the solder joints because of the lack of buoyancy force was suggested but not confirmed [2]. Jones and deRooij [3] reported that there was no observed difference between solder joints produced in reduced-gravity on a research aircraft and under normal $1g$ conditions from the standpoint of internal microstructure. They did not, however, report on other functional characteristics of the solder joints.

A manual soldering test was performed on Shuttle mission STS-57 in 1993. In this test a variety of types of solder joints were produced.

Although there was no report of detailed analysis on the characteristics of these samples, the success of this test was sufficient to warrant manifesting a soldering kit on ISS for contingency repairs.

To gain confidence in the reliability of soldering as a standard repair process for space missions, we conducted a more detailed assessment of the important service-related characteristics of solder joints produced in low-gravity. As a preliminary step in this effort, beginning in 2001, we conducted a series of reduced-gravity soldering tests using KC-135 research aircraft. The testing involved eight flight weeks and spanned over three years, using a plated through-hole (PTH) configuration. Results of these tests characterized changes in the solder joints, including geometric changes and increases in internal porosity as a result of the reduced-gravity environment. The sources of the increased porosity appear to be flux vapor which was trapped in the molten solder, and entrapped moisture in the circuit board itself. Several techniques were tested to mitigate the porosity increase, including alternate techniques for flux application and demoisturization of the circuit board before soldering.

II. Experimental Procedure

Soldering operations took place onboard a KC-135 reduced-gravity research aircraft. This aircraft flies repeated parabolic trajectories yielding 20–30 s periods of reduced gravity of approximately $10^{-2} g_e$ (where $1 g_e$ is the normal gravitational acceleration of about 9.8 m/s^2 experienced on earth at sea level). This aircraft is also capable of flying modified parabolic trajectories that yield partial-g environments such as those experienced on the surface of the moon or Mars. Although most reduced-g samples in this project were produced in a nominal $10^{-2} g_e$ environment, a limited number were produced at accelerations of $0.1 g_e$, $0.17 g_e$ (lunar), $0.25 g_e$, and $0.38 g_e$ (Mars). The actual acceleration achieved onboard the aircraft may not be precisely the nominal value and is also subject to irregular disturbances from pilot control inputs, atmospheric buffeting, and other sources. During each parabola, the space acceleration measurement system (SAMS) hardware, located on our experiment, measured and recorded the acceleration at 100 Hz in the three primary orthogonal axes of the aircraft [4]. The quality of each parabola was assessed in terms of disturbances to the reduced-gravity environment [5]. Baseline samples soldered under $1 g_e$ conditions were made in the experimental hardware on the aircraft: both on the ground (atmospheric pressure approximately 0.10 MPa) and in flight at a cabin pressure of roughly 0.08–0.09 MPa.

Manual soldering was performed on samples composed of 1/2 W carbon resistors mounted to the PTH printed circuit board (PCB). The soldering iron is a Weller® model TCP 12P with a PTP7 tip and is similar to that currently flown in the soldering kit aboard the ISS. The same PCB configuration (Fig. 1) was used throughout the tests; however, two different resistor diameter leads (0.66 mm and 0.78 mm ± 0.04 mm) were used. Before soldering, the samples were prepared (e.g., cleanliness, tinning, etc.) according to the NASA standard for electrical connections [6]. However, only some of the boards were demoisturized (by an oven bake) before soldering. The resistors and PCBs were preassembled, with the resistors held in position by a silicon rubber adhesive. Resistor leads, which were tinned with solder (60/40 wt% Sn/Pb), were inserted through a 1.33-mm-diam plated through-hole. For each joint, solder wire was precut and weighed before and after soldering to estimate the mass added to each joint. The soldering of all samples was videotaped with sufficient resolution to observe the details of soldering such as pre- and postheat times as well as solidification. In some cases, pre- and postheat times were controlled. A pressure transducer provided ambient pressure measurements and select samples were instrumented with thermocouples providing temperature measurements during the soldering process. Additionally, a relative humidity reading was manually recorded during soldering for a significant portion of the tests. More detail of the experimental hardware is provided elsewhere [7,8].

For reasons to be discussed later, several variations of the soldering procedure were tested. These included 1) 60/40 wt% Sn/Pb rosin core solder, PCBs in as-received condition from the manufacturer; 2) 60/40 wt% Sn/Pb, rosin core solder, PCBs baked at least 4 h at 93°C and subsequently kept in a dry environment before soldering; 3) 60/40 wt% Sn/Pb, solid solder, externally applied liquid flux (Multicore 6381–25), PCBs in as-received condition; and 4) 60/40 wt% Sn/Pb, solid core, externally applied gel flux (Kester RF-741), PCBs in as-received condition.

Seven individuals performed the soldering operations. These personnel were provided with training to assure a common base level of knowledge and experience. Two of the individuals are certified for soldering of spaceflight hardware per NASA standards and, thus, were considered to be "experts." This provided a range of skill levels, from "trained-novice" through expert, such as may be encountered on a flight crew.

Following cleaning of residual surface flux, all samples were visually inspected (pass/fail) to the applicable NASA standard [6]. Additional post-soldering evaluation of the samples included geometrical measurements and metallographic cross-sectioning and examination. More detail is provided in the following section.

The primary macroscopic geometrical characteristic of interest was fillet leg length, as defined in Fig. 2a. The values of the vertical leg lengths were measured from images of the sample profiles before cross-sectioning. The vertical fillet leg length on the side of the joint to which the solder alloy was added (i.e., the top) was designated as L_T. Conversely, the fillet leg length on the other side of the PCB (i.e., the bottom) was designated as L_B.

The subsequently cross-sectioned fillets revealed features of interest that were visible without additional processing. Cross sections were photographed at approximately 20× magnification (Fig. 2b). Internal porosity (or void content), as a percentage of cross-sectional area, was determined by digitizing the photographs (Fig. 2c) and electronically designating the voids (the area shown in gray) and the entire area of solidified solder alloy (the sum of the areas shown in gray and white). This procedure and the subsequent data analysis are in accordance with ASTM Standard E1245-00 [9].

III. Results and Discussion

To date, we have generated 1347 solder samples in the plated through-hole configuration, including 938 low-gravity samples

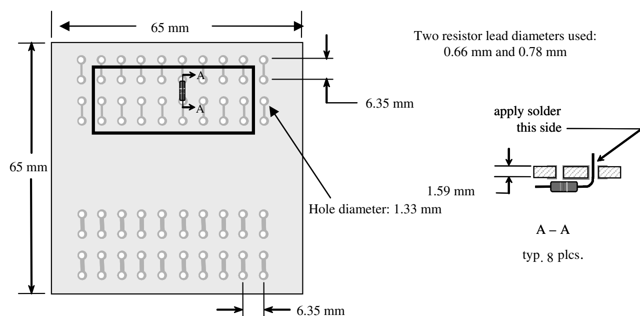

Fig. 1 Sample configuration. All dimensions are approximate.

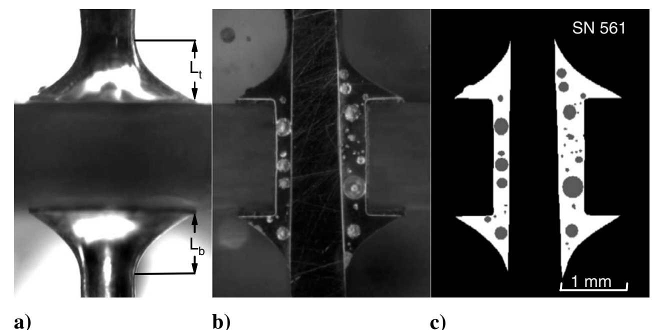

Fig. 2 Images of joints a) after soldering in reduced gravity, b) after cross-sectioning, and c) after computer analysis.

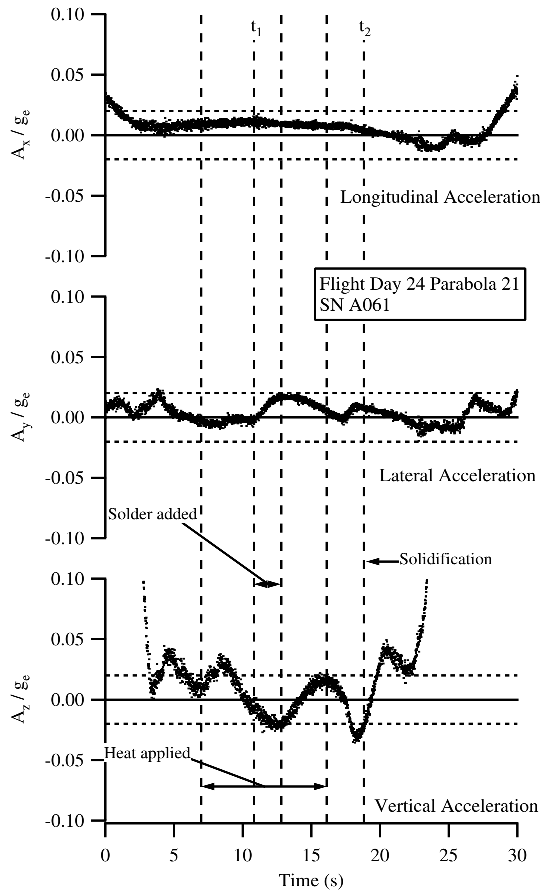

Fig. 3 Acceleration data from the SAMS three-axis accelerometer taken while soldering a PTH joint during a targeted $0g_e$ parabola [5].

(with some partial-gravity samples) and 409 normal-gravity samples. Two different resistor lead diameters were used in the experiment: 0.66 and 0.78 mm. The varying lead diameters produce different gap widths for the solder to flow through. This varying gap width may affect the capillary forces that move the fluid in microgravity. For the present analysis, however, we did not differentiate samples with different resistor lead diameters.

A. Acceleration Environment

The acceleration experienced onboard the aircraft is subject to a variety of changing conditions. These include irregular low-frequency, high-amplitude disturbances from pilot control inputs, atmospheric buffeting, and other sources, as well as high-frequency, low-amplitude vibrations (termed "g-jitter") from airframe, and engine vibrations. These undesired accelerations cause both low- and high-frequency oscillations about the targeted acceleration level. A recent paper, which describes the acceleration environment and measurements in detail, investigated the influence of g-jitter on the soldering process, particularly porosity [5]. Based on results of this paper, we established an acceptance criterion of $A \leq 0.02g_e$ during the time when the solder was molten. The equation used to compute A is shown in Eq. (1) and represents the time-averaged magnitude of the three-dimensional acceleration for each parabola using the root-sum-square (RSS) method. In Eq. (1), the symbols A_x, A_y, and A_z are the magnitude of acceleration in the longitudinal, lateral, and vertical axes of the aircraft, respectively, whereas t represents time. An example of the acceleration data obtained during a test is shown in Fig. 3. The horizontal lines on each graph denote acceleration values of $\pm 0.02g_e$ whereas the vertical lines denote events during the soldering process which are labeled in the figure. In Fig. 3, the solder is molten from t_1 to t_2 and the integration in Eq. (1) yields an acceptable parabola with the value of A being $0.02g_e$. With the exception of leg-length data, all nominally $0g_e$ data presented only include cases that passed the g filter (i.e., $A \leq 0.02g_e$). Finally, partial-gravity parabolas (i.e., $0.1g_e$, lunar $0.17g_e$, or Martian $-0.38g_e$) were also unfiltered.

$$A = \frac{1}{t_2 - t_1} \int_{t_1}^{t_2} \sqrt{A_x^2(t) + A_y^2(t) + A_z^2(t)}\, \mathrm{d}t \qquad (1)$$

B. Visual Examination

All samples were visually inspected to the applicable NASA standard [6]. Results of the visual inspection are presented in Table 1. The causes for failure during the inspection have been categorized as either "surface porosity" or "workmanship." In this context the term surface porosity includes any feature that is indicative of porosity in the solder joint. Examples would include pores or pinholes obviously open to the surface, cavities interpreted as being collapsed bubbles, and bulges or spikes interpreted as being closed bubbles manifested at the surface. The term workmanship includes lack of wetting of the solder alloy, lack of flow-through of solder alloy from the side of the joint to which it is applied to the other side, insufficient or excess solder, indications of overheating, or visible contaminants. The data in Table 1 indicate that a larger percent of joints failed due to surface porosity across all conditions in $0g_e$ when compared with $1g_e$. The data suggest that there is a lower incidence of workmanship failures for samples produced in $0g_e$ compared with those produced in $1g_e$. Finally, no noteworthy differences were seen in the quality of samples produced by the experienced soldering technician compared with the samples produced by less-experienced personnel. This was true for both the visual inspection failures presented here and also the quantity of porosity which is discussed in the next section.

C. Internal Porosity

1. Volume Fraction of Porosity as a Function of g-Level for Plated Through-Hole Soldering

Joint porosity is defined as the ratio of 2-D areas designated as voids (shown in gray in Fig. 2c) to the 2-D imaged area of solidified solder alloy (white and gray areas). The relationship between a void volume fraction measured at one planar location and the volume fraction of the entire joint may not be valid for any single joint, unless the voids are uniformly distributed throughout the joint. However, large population statistics (i.e., planar measurements over many joints) can reasonably represent the average nature of the void distribution throughout the joint [9].

Figure 4 shows a plot of the cumulative fraction of samples that have a given porosity or less. The data in Fig. 4 compare joints that were formed in near $0g_e$ to those formed in $1g_e$ using flux-cored solder. For example, this plots shows that 80% of the normal-gravity samples have roughly 4% or less porosity, whereas only about 33% of the low-g samples have similar porosity.

Table 1 Percentage of samples failing visual inspection for each test condition

Soldering conditions	Total samples $1g_e/0g_e$	Surface porosity % failed (no. failed)		Workmanship % failed (no. failed)	
		$1g_e$	$0g_e$	$1g_e$	$0g_e$
Flux-core solder	102/77	11.8% (12)	19.5% (15)	5.9% (6)	7.8% (6)
Solid solder–liquid flux	111/153	5.4% (6)	15.0% (23)	12.6% (14)	7.2% (11)
Solid solder–gel flux	32/43	9.4% (3)	44.2% (19)	15.6% (5)	2.3% (1)
Flux-core solder, baked PCB	56/102	0.0% (0)	4.9% (5)	16.1% (9)	2.0% (2)

Table 2 Mean porosity values for partial-gravity samples

Test condition	$0g_e$	$0.10g_e$	$0.17g_e$ (lunar)	$0.38g_e$ (Martian)	$1g_e$
Flux-core solder	11.0 ± 2.38% 77 samples	9.27% 11 samples	7.75% 16 samples	5.41% 18 samples	3.21 ± 1.17% 102 samples
Solid solder–liquid flux	6.64 ± 1.24% 153 samples	n/a	6.44% 7samples	8.53% 7 samples	2.75 ± 0.64% 111 samples
Solid solder–gel flux	10.5 ± 2.40% 43 samples	n/a	n/a	n/a	3.44 ± 1.57% 32 samples
Flux-core solder, baked PCB	6.32 ± 1.40% 102 samples	1.43% 5 samples	3.80% 5 samples	5.47% 10 samples	2.78 ± 1.54% 56 samples

A limited number of samples were produced in partial-gravity environments. The acceleration environment for these tests was nominally $0.10g_e$, $0.17g_e$ (lunar), or $0.38g_e$ (Martian), ± approximately $0.02g_e$ for each case. The sample populations were small for each test, both because of the limited number of partial-g parabolas performed on each flight (typically, a maximum of 5–10 of the ∼40 parabolas per flight are flown in a partial-g profile, if any), and because the number of available partial-g parabolas was divided between different soldering techniques. These tests were mainly conducted using flux-core solder with PCBs in either as-received condition or baked, though a small number were tried with solid solder and liquid flux.

Table 2 shows the porosity data from the partial-gravity tests, along with results from (nominally) $0g_e$ tests, for comparison. The 95% confidence intervals on the mean values were not computed for the partial-gravity data sets due to the comparatively small populations. The small number of samples in each given condition precludes meaningful statistical comparisons of the partial-g results, but the general trend (with regard to the mean porosity percentage) suggests the expected result that porosity increases as the acceleration levels decrease. Further testing at these conditions would be required to develop a data set of sufficient size to draw definitive conclusions.

2. *Causes and Impact of Porosity*

Porosity in solder joints likely comes from entrapped gasses which are composed of vaporized flux and/or water vapor. A decrease in gravity reduces the buoyancy force allowing fewer bubbles to escape to the surface. Previous analysis has suggested that the small bubbles in solder reach their terminal velocity within milliseconds [5]. This same analysis shows that for a typical bubble with a radius of 0.075 mm the terminal velocity drops from 6 mm/s in $1g_e$ to 0.1 mm/s at $0.02g_e$. This implies that for distances characteristic of the samples used in this experiment and for the periods of time for which the solder is molten, there is likely inadequate time for the majority of pores to move to a free surface and dissipate. Further, because the disturbances to the gravitational environment onboard the aircraft have a variable direction, bubble motion will not be steady in one direction for the total available time, but, rather, will be briefly in one direction then in another. This type of motion is believed to promote retention of bubbles. Bubble motion is expected to be even slower in true microgravity environments aboard spacecraft, thus further promoting bubble retention.

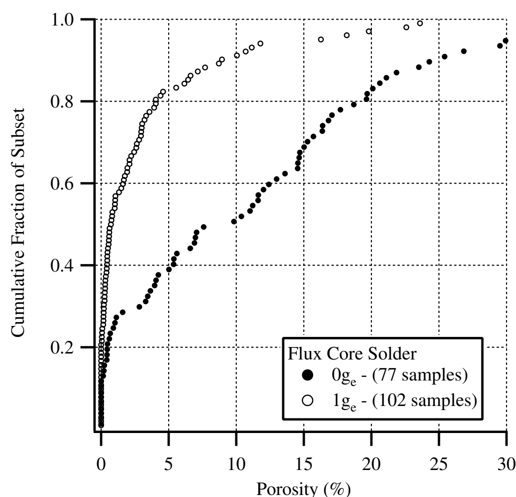

Fig. 4 Cumulative distribution function for porosity of flux-cored solder joints [5].

Consistent with the results reported here, recent experiments performed by the Imperial College of London on a research aircraft with a Sn-Ag-Cu eutectic solder alloy showed large increases in volume fraction of porosity in samples produced in $0g_e$ compared with those produced in $1g_e$, also attributed to lack of buoyant forces on bubbles formed by vaporized flux.[‖] Mechanical testing of the $0g_e$ samples yielded a shear strength of 15.5 ± 2 MPa: almost 30% less than the 22 MPa demonstrated by samples produced in $1g_e$. Thus, it is important to develop techniques to mitigate the increase of porosity in reduced gravity.

The second most likely source of the gas that produced the porosity (following the solder flux) is absorbed moisture within the PCB material that diffuses through the plating on the surface of the hole and into the liquid solder alloy. It is known that epoxy-glass laminate materials used for PCB substrates can absorb significant amounts of moisture even under conditions of modest temperature and humidity [10]. This absorbed moisture has been credited as a source of porosity in solder joints [11].

3. *Porosity Mitigation Techniques*

Because both entrapped flux and moisture evolved from the PCB are potential sources of porosity, experiments were performed to explore alternative fluxing techniques in an effort to reduce porosity and to assess the contribution to porosity from moisture. The first porosity mitigation technique tested was to apply a liquid flux (Multicore 6381-25) to the joint, heat the joint for sufficient time (discussed subsequently) to activate the flux and allow a significant amount of it to dissipate, and then apply the solid-core solder alloy before reoxidation of the joint. A slight modification of this technique was to employ a gel flux (Kester RF-741) rather than the liquid flux. We believed that the gel flux might be easier to apply to the joint in operational on-orbit conditions. To maximize the available time for soldering, we applied the solder flux during the $2g_e$ pull-up just before the reduced-gravity portion of a parabola on the KC-135 aircraft. The application of flux during $2g_e$ allowed the flux to preferentially move through the through hole. We did a limited number of flux-application tests in $0g_e$ and observed that flux was drawn though the through hole sufficiently for our geometry and wetted the bottom side of the solder pad (although not in as great a quantity as seen in $2g_e$).

During a portion of the testing, we loosely controlled the pre- and post-heat durations. This was done to see if we would observe any changes in joint porosity and perhaps ascertain optimum pre- and post-heat durations. Finally, select PCBs were baked and kept in a desiccated environment before soldering to assess the effect of absorbed circuit board moisture on joint porosity.

a. Liquid Flux with Solid-Core Solder. The cumulative distribution functions for samples produced with externally applied

‖Data available on-line at http://www.estec.esa.nl/outreach/parabolic/results_2003_frame.htm [cited 28 Oct. 2005].

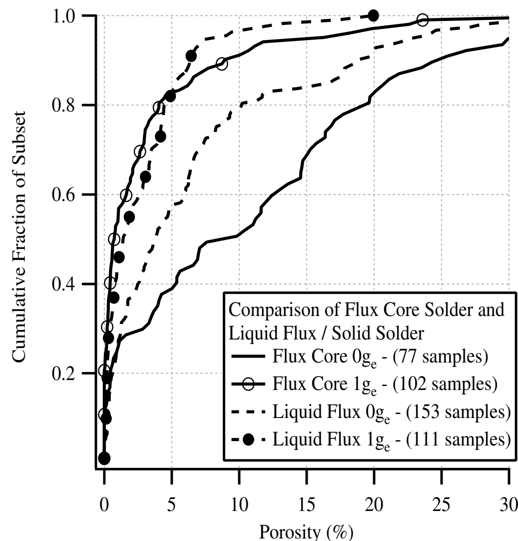

Fig. 5 Cumulative distribution function for porosity of joints made with flux core and liquid flux/solid core solder.

liquid flux and solid solder wire are shown in Fig. 5. Included in this figure, for comparison, are the cumulative distribution functions for samples produced with conventional flux-cored solder.

From this figure it can be seen that for samples produced under $1g_e$ acceleration, the two soldering methods yielded similar results. At reduced acceleration, however, the samples produced with externally applied liquid flux contained significantly less porosity than samples produced with flux-cored solder.

b. Gel Flux with Solid-Core solder. The cumulative distribution functions for samples produced with externally applied gel flux and solid solder wire are shown in Fig. 6. Included in this figure, for comparison, are the cumulative distribution functions for samples produced with conventional flux-cored solder.

Again, it is evident that for samples produced under $1g$ acceleration, the two soldering methods yielded similar results. At reduced acceleration, however, the samples produced with externally applied gel flux are only marginally better than samples produced with flux-cored solder. This suggests that, at least for this specific gel-flux, the technique employed did not result in sufficient dissipation of the flux to substantially reduce porosity.

c. Effect of Pre- and Post-Heat Time. During portions of the experiment, we loosely controlled the pre- and post-heating times. Nominally, we chose both pre- and post-heat intervals of 3 and 6 s which we deemed as optimal and slightly excessive, respectively.

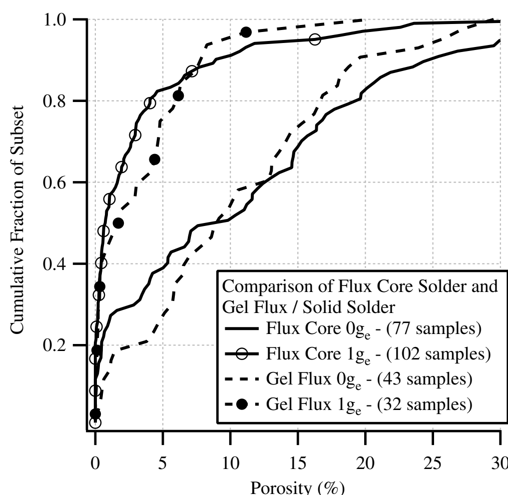

Fig. 6 Cumulative distribution function for porosity of joints made with flux core and gel flux/solid core solder.

Table 3 Effect of preheat duration on joint porosity in $0g_e$ conditions

Soldering conditions	Preheat: 3 ± 1 s Post-heat: 3 ± 1 s	Preheat 7 ± 1 s Post-heat: 3 ± 1 s
	Porosity (samples)	Porosity (samples)
Solid solder–liquid flux	6.43 ± 2.86 (28)	6.18 ± 4.57 (14)
Solid solder–gel flux	10.89 ± 4.39 (10)	10.19 ± 4.53 (16)

Although pre- and post-heat times were not precisely controlled, actual heating times for each test were extracted through video analysis. Data from tests where the timing was not specifically controlled but did fall into a desired interval were included in the subsequent analysis.

For cases of externally applied flux, we believed that variations in preheat time might influence joint porosity. For example, we conjectured that in a case of low preheating not all of the flux would be vaporized and consequently a larger porosity might occur. Based on the heating time distributions for the $0g_e$ samples with externally applied flux, we generated two data sets for comparison: those with preheating of 3 ± 1 s and 7 ± 1 s. For preheat time comparison, the data sets were restricted to samples where the post-heat time is in the range of 3 ± 1 s. The intent was to isolate any effects of the preheat time by holding the post-heat time quasi-constant. The results for this analysis are summarized in Table 3. These results show no statistical difference between the selected preheat times.

We investigated several other groupings of pre- and post-heat times in both $0g_e$ and $1g_e$; however, no clear effect on the sample porosity emerged. In most cases, the number of samples in the data subsets was low, resulting in rather large uncertainty. In the cases where the data subsets contain a larger number of samples, we observed no statistical difference in the porosity values as a result of preheat or post-heat time variations in this experiment.

d. Printed Circuit Board Moisture Removal. The question arises as to why there is porosity in $1g_e$ samples if buoyancy is truly effective in causing bubbles to move to a free surface and be expelled. The likely answer is related to the sources of porosity and heating time. The introduction of flux ends either before the application of the alloy (in the case of the externally applied flux) or concurrently with the end of introduction of alloy (in the case of flux-cored wire). There follows a period of continued heating with the soldering iron to ensure distribution of the solder alloy and a period of progressive solidification. During this time the bubbles within the molten metal arising from vaporized flux can move to free surfaces and dissipate. The other source of porosity is the moisture that evolves from the PCB laminate [10]. For the soldering period, evolved moisture is probably a somewhat continuous source, introducing porosity into the solder alloy throughout the time during which it is molten. It is probable that moisture introduced into the molten alloy immediately before solidification does not have adequate time to move to the free surfaces and is trapped within the joint.

To remove entrapped moisture, select PCBs were baked before soldering as per NASA-STD-8739.3. This process required baking the PCB at a temperature of 93°C for a minimum of four hours. The PCBs for this experiment were typically baked overnight for a period of approximately 16 h. Measurements of the PCB mass were made before and after the demoisturization process. These measurements indicated that the average mass lost per board was 0.036 ± 0.003 g where the error bar represents 1 standard deviation. For an average board mass of 14.5 grams, this represents a 0.25% decrease in mass as a result of the demoisturization process. The likely source of this lost mass is absorbed water in the laminate material of the PCB (although strictly speaking we did not rule out the possibility of some other material evolving from the laminate). We performed a test wherein demoisturized PCBs were stored in environments of different relative humidity. The results of this test showed that a PCB exposed to normal room humidity (~40%) regained only about 8% of its lost mass in 20 min which is roughly the maximum duration a board would be removed from the desiccated environment before soldering during our tests. PCBs stored in this normal room environment eventually regained 33% of their lost mass after seven

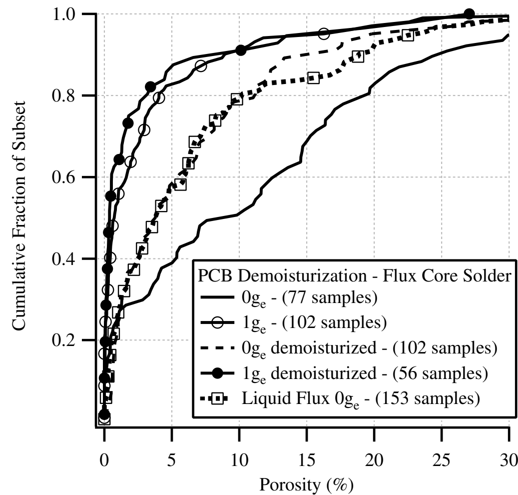

Fig. 7 Cumulative distribution function showing effect of baking the PCB at 93°C for 4 h.

days. The humidity levels aboard the KC-135[¶] are typically lower than the normal room environment indicating that we were, in fact, soldering demoisturized boards during our experiment. As a corollary to this test, we exposed baked PCBs to 100% relative humidity. These boards regained ~14% of their lost mass within 20 min. The boards stored in a saturated (100% relative humidity) environment eventually gained up to 0.090 g of mass (or 251% of their lost mass). This suggests that mass lost during the demoisturization process can be replaced (or even exceeded) with water absorbed from the surrounding environment.

PCB bakeout does reduce the overall porosity of the joint (Fig. 7). Included in this figure, for comparison, are the cumulative distribution functions for samples produced with conventional flux-cored solder. Examination of solder joints made with demoisturized PCBs shows that the positive effect on porosity reduction achieved by removing moisture from the boards is similar to those achieved using the liquid flux which is also included in Fig. 7.

4. *Pore Size Distribution as a Function of g-Level*

Data for the average pore diameter and the average number of pores seen in sample cross sections are presented in Table 4. We were able to resolve pore diameters as small as ~0.012 mm. The uncertainty of the mean pore diameter in Table 4 represents a 95% confidence interval on the mean value. Pore diameters are stated as they appear in cross section images. Because of the arbitrary location of the cross-sectioning plane with respect to the internal pores, the true pore diameters are almost certainly larger than they appear, except in the unlikely event that a joint's cross section image coincides exactly with the center of a pore. Whereas the relationship between apparent and actual pore diameter is not readily quantifiable, it is assumed that for large sample populations this effect acts similarly on each population. Thus, the resulting numbers are only useful for comparison with other sample populations and do not represent accurate pore diameter measurements.

Similarly, it is unlikely that every pore in a joint would be visible in a single cross section. Using the same argument, it is assumed that these results are useful for comparison among different subsets of data, but do not likely represent the actual number of pores in a given joint.

The data in Table 4 show that pore diameters, on average, are smaller in $1g_e$ when compared with $0g_e$. Also, the number of pores per joint decreases in $1g_e$ when compared with $0g_e$. This reduction is also apparent in the confidence intervals, which increase for $1g_e$. The reduced number of pores per joint for the $1g_e$ samples is likely due to buoyant forces which have expelled a significant number of bubbles. Similarly, the larger bubbles in $1g_e$ are more likely to reach a free surface owing to their larger buoyantly induced velocity.

5. *Correlation of Visual Inspection Results with Measured Porosity*

External visual inspection is the only method of quality assurance currently available to crew members. Consequently, verifying the effectiveness of using external inspection to determine internal qualities of soldered connections is of relevance to this undertaking. To determine whether visual inspection is an adequate indicator of internal solder joint quality, internal porosity metrics (average volume percent porosity, average pore diameter, and average number of pores per joint) were tabulated for groupings of visual inspection results. Samples from all soldering process variations (flux-core solder, liquid flux, gel flux, and baked boards) were grouped together under the assumption that the relationship between external appearance and measured porosity would be independent of solder/flux type. The results of this comparison are presented in Table 5. The uncertainties in the tabulated results reflect statistical confidence intervals at the 95% confidence level.

The data in Table 5 show that all $0g_e$ subsets had (on average) greater porosity, larger average pore diameters, and increased number of pores per joint than the respective $1g_e$ subset although low-sample numbers in some cases make the 95% confidence intervals high. Within the $0g_e$ subset, samples that failed the inspection due to surface porosity had significantly higher porosity values and average pore diameters than either of the other two groups of $0g_e$ samples. The same can be said of the $1g_e$ samples, although the low number of failing joints due to surface porosity (21) resulted in large confidence intervals (hence greater uncertainty) for that condition. Interestingly, the $0g_e$ subset of samples that passed the visual inspection had joint porosity values similar (statistically) to those which failed the visual inspection in $1g_e$. A reasonable explanation for this is that the bubbles in the $0g_e$ samples are moving at very low velocities and, thus, are predominantly located in the interior of the joint at the time of solidification. In contrast, the bubbles in the $1g_e$ samples are moving rapidly towards the free surface so that those which remain at the time of solidification are more likely to be at or near the surface. Nonetheless, the generalization can be made that, on average, samples with external indications of internal porosity (cavities, pinholes, bulges, etc.) have higher porosity than samples lacking these indications. Thus, a visual inspection can be a useful tool (particularly because of its inherent simplicity) to determine whether a solder joint contains excess porosity.

6. *Pressure Effects*

To assess the potential influence of reduced aircraft cabin pressure when soldering at altitude, we compared data sets for two sets of soldering conditions: those produced onboard the aircraft while it was aloft at a nominal acceleration value of $1g_e$ and while it was stationary on the ground. The atmospheric pressure of the aircraft cabin, while flying, is maintained at the equivalent of that at approximately 2400 m altitude (0.08–0.09 MPa). The mean number of pores and the mean apparent pore diameter were determined for the sample sets. Results are shown in Table 6.

The data indicate that, in general, for both soldering conditions, the mean number of pores is greater when soldering occurred at the reduced pressure experienced during flight. However, because the sample populations examined were rather small and the confidence intervals are commensurately large, a firm conclusion that reduced pressure increases number of pores is not possible. It is possible that reduced pressure has a positive effect on nucleation of bubbles forming from moisture originating in the PCB laminate. The presence of flux from which flux-based pores form should be independent of ambient pressure. The data suggest that the ambient pressure does not have a significant effect on average pore diameter,

[¶]For the $0g_e$ samples, the average recorded relative humidity in the glovebox was 26.6% with a standard deviation of 11.1% (651 samples). For the $1g_e$ samples, the average recorded relative humidity in the glovebox was 51.6% with a standard deviation of 18% (227 samples). Please note that the relative humidity was a manual measurement and was not recorded for every sample.

Table 4 Pore size distribution as a function of g-level and soldering condition

Condition	$0g_e$			$1g_e$		
	Mean pore diameter, mm	Mean pores per joint	Samples	Mean pore diameter, mm	Mean pores per joint	Samples
Flux core	0.108 ± 0.005	18.0	77	0.070 ± 0.007	6.5	102[a]
Solid core/liquid flux	0.103 ± 0.005	13.1	153	0.069 ± 0.005	8.5	111[a]
Solid core/gel flux	0.097 ± 0.007	21.1	43	0.066 ± 0.009	11.9	32[a]
Flux core/baked board	0.088 ± 0.006	11.2	102	0.073 ± 0.011	5.8	56[a]

[a]Includes $1g$ samples soldered on the ground and at altitude (0.08–0.09 MPa cabin pressure).

Table 5 Joint porosity characteristics sorted by visual inspection results; all soldering conditions represented

g-level	Data subset	Samples	Average porosity, %	Average pore diameter, mm	Average pores/joint
$0g_e$	Passed visual inspection	293	7.24 ± 0.92	0.097 ± 0.003	14.0 ± 1.6
	Failed—workmanship	20	5.42 ± 3.64	0.089 ± 0.016	9.8 ± 4.4
	Failed—surface porosity	62	11.76 ± 2.42	0.113 ± 0.007	18.2 ± 4.0
$1g_e$	Passed visual inspection	246	2.91 ± 0.60	0.067 ± 0.004	8.2 ± 1.4
	Failed—workmanship	34	1.76 ± 0.87	0.075 ± 0.015	4.6 ± 1.7
	Failed—surface porosity	21	5.88 ± 3.56	0.105 ± 0.021	7.1 ± 2.7

Table 6 Influence of altitude and cabin pressure on internal porosity in normal gravity

	Condition	Number of samples	Mean number of pores (±95% CI)	Mean pore diameter ±95% CI, mm
Flux-core solder	Ground[a]	70	6.4 ± 2.3	0.069 ± 0.009
	Altitude[b]	32	6.7 ± 2.2	0.073 ± 0.01
Solid-core solder, liquid flux	Ground[a]	103	8.8 ± 2.7	0.068 ± 0.005
	Altitude[b]	8	5.0 ± 3.9	0.109 ± 0.038
Solid-core solder, gel flux	Ground[a]	16	10.4 ± 3.1	0.066 ± 0.015
	Altitude[b]	16	13.5 ± 8.3	0.067 ± 0.013
Flux-core solder, demoisturized boards	Ground[a]	24	3.3 ± 1.0	0.073 ± 0.021
	Altitude[b]	32	7.6 ± 2.2	0.073 ± 0.010

[a]Soldering performed on ground at atmospheric pressure of approximately 0.10 MPa. [b]Soldering performed while aircraft at altitude with a cabin pressure of 0.08–0.09 MPa.

though we note that the pressure range considered was quite narrow (0.08–0.10 MPa,).

D. Cooling Rate

The crew member who conducted the manual soldering experiment aboard STS-57 in 1993 reported to the authors that the solidification time appeared to be longer for joints soldered in microgravity (compared with those he soldered on Earth while training). If this observation is correct, then the likely reason for this difference is the lack of buoyancy-driven convection available to contribute to heat loss from the exposed surface of the solder joint. To help understand any differences in cooling rate, we instrumented several of our solder samples with small type K thermocouples (0.051 mm diameter wire and ∼0.17 mm beads). The thermocouples, which were spot-welded to the metal pad on the surface of the PCB, recorded temperature data during the soldering process (Fig. 8). A small number of these instrumented samples included a second thermocouple at another location. The purpose of this additional thermocouple was to determine if temperature gradients existed across a joint; the resultant data (not shown) indicate that the temperature of these joints was essentially spatially uniform. Using these data, the temperature profiles and heat transfer rates in both reduced-gravity and normal-gravity environments were analyzed and compared statistically. In Fig. 8, the vertical lines on the chart correspond to events in the soldering process as labeled. These times were determined from the videos. Note that the right-most vertical line corresponds to when the joint is completely solidified, which was visually manifested in the videos as a change in luster. The joint temperatures measured by thermocouple correlated well with the observations of soldering events on the video data (e.g., heat application, heat removal, and solidification).

As the time required for a joint to solidify depends on several factors (such as joint mass and peak temperature), a comparison of cooling time only is not meaningful. Rather, the average rate of heat transfer during the cooling period is computed for each joint as follows. The total thermal energy lost by the solder in the course of cooling from the peak temperature through solidification is shown in Eq. (2). This equation assumes that the joint temperature is spatially uniform and that the specific heat is independent of temperature. The thermophysical properties are listed in the nomenclature. In Eq. (2), the mass of the solder joint was determined by weighing the solder feed wire before and after soldering.

$$Q = mC_p(T_p - T_m) + mh_f \tag{2}$$

To determine the average heat transfer rate from the solder joint, the total energy is simply divided by the cooling time as shown in Eq. (3). The cooling time was determined from data like that shown in Fig. 8 and represents the time from solder iron removal to complete joint solidification (as determined from the end of the plateau region seen in the figure).

$$\dot{Q}_{\text{av}} = \frac{Q}{t_c} \tag{3}$$

The results of this computation are given in Table 7 in the form of an average heat transfer rate across all instrumented samples for each data subset. The computation of the confidence intervals assumes a t-student distribution.

The data in Table 7 show that the heat transfer from the solder joints is slightly slower in $0g_e$ than in $1g_e$. This supports the idea that joints will take longer to solidify in reduced gravity due to a lack of natural convection. Because of small sample populations and consequently large confidence intervals, though, it cannot be said that the joint cooling rates are statistically different in reduced gravity above a calculated confidence level of 60%. Nevertheless, if the nominal average heat transfer rates truly are representative, then the solidification time of $0g_e$ and $1g_e$ samples of the same mass would be approximately 10%, or slightly less than 0.5 s. Although this is a

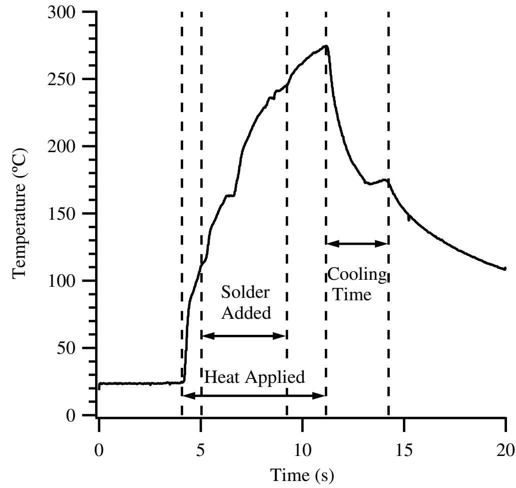

Fig. 8 Typical thermocouple and video data plot for the soldering process. The dashed lines represent soldering events as determined from the videos.

fairly small difference, it would be visually detectable and could account for the observation of the STS-57 crew member.

E. Leg-Length Geometry

The overall geometry of a PTH solder joint is affected by body forces (due to mass and gravity) and surface tension forces acting on the joint while the solder is molten [12–15]. In a previous paper [16], we have observed that geometrical differences exist in solder joints produced in reduced gravity, as compared with those formed in normal gravity. Those results, along with the average solder mass added data, are repeated here for completeness. A measure of the joint geometry is the ratio of leg lengths, L_T (top leg) to L_B (bottom leg), as shown in Fig. 2a. The leg lengths were measured using digitized, magnified images of the complete solder joint (before cross-sectioning). The resulting mean leg-length ratios for various test conditions are shown in Table 8. The mass of solder added was determined by weighing precut pieces of solder used to make the joints, then reweighing them afterward. The uncertainties listed in Table 8 reflect a 95% confidence interval on the mean value assuming a *t*-student distribution and the individual measurement uncertainties of each sample. More details regarding the data set are in [16].

The average amount of mass added for joints formed with flux-core solder were indistinguishable between normal and reduced gravity, within the limits of the 95% confidence interval. However, slightly more solder was added with the solid core/liquid flux combination (about 10–15%). Further, more solder was added when using the solid core/liquid flux technique than with the flux-core solder, although the reasons for this are not clear.

Whereas normal gravity joints have mean leg-length ratios significantly less than unity, the same ratio for reduced gravity joints tended to slightly exceed unity. The trends held similarly for both the flux-cored solder and the solid solder/liquid flux combination. Whereas the previously noted increase in mass added (in the case of the solid-core solder/liquid flux) could account for some portion of the increase in the leg-length ratio, this increase occurred even when similar amounts of mass were added (as in the case of the flux-core solder). This implies that the changes in the leg-length ratio are not simply due to changes in mass added, though additional mass would also tend to increase this effect. The hypothesized reason for the increased leg-length ratio in reduced gravity is that there is insufficient time or driving force before solidification to transport the solder from the top to the bottom of the joint. However, other effects such as bubble evolution and solder application technique tend to confound the joint equilibration.

Comparison of the relative importance of body forces versus surface tension forces can be studied by examining the Bond number [Eq. (4)].

$$Bo = \frac{\rho g L^2}{\sigma} \tag{4}$$

For the PTH geometry in normal gravity, the coupling of the top and bottom fillet suggests that a relevant length scale is the board thickness (~1.6 mm). Using this length scale, the Bond number is on the order of 1, meaning that body forces are similar in magnitude to the surface tension forces. Because the Bond number scales with gravity, it will be on the order of 10^{-2} for the reduced-gravity tests in this study, indicating that surface tension forces become more important in those cases. The expectation would then be that these joints would be symmetric, lacking a driving force which would distort them. This is supported by the observed leg-length ratios, which are much closer to unity in reduced gravity than in normal gravity. The fact that the ratios are greater than 1 for the reduced-gravity cases can be explained by the previously mentioned solidification argument, and also potentially by the small additional mass added in reduced gravity for our tests.

Table 7 Average overall heat transfer rates for normal- and reduced-gravity subsets

	Number of samples	Average heat transfer rate ($\mu \pm$ 95% CI)	Average heat transfer rate ($\mu \pm$ 60% CI)
Low-*g*	31	0.67 ± 0.09 W	0.67 ± 0.04 W
1*g*	25	0.75 ± 0.11 W	0.75 ± 0.11 W

IV. Conclusion

Experimental efforts have demonstrated that manual soldering is a viable process for repair of electronic systems as an element of in-flight maintenance capabilities. Although the reduced-gravity environment introduces some new issues, these can be accommodated by appropriate application of modified processes and alternative materials used in the soldering process. Specific findings of this study are enumerated as follows:

1) Solder joints produced in a $0g_e$ environment with conventional soldering techniques (using solder wire with a flux core) typically exhibit significantly higher levels of porosity than joints soldered in a $1g_e$ environment.

2) Sources of porosity in solder joints include flux which vaporizes to form bubbles and moisture that is evolved from the PCB laminate. In a $0g_e$ environment the lack of buoyant forces results in slower bubble transport and eventual entrapment as pores upon freezing of the solder alloy.

3) Porosity resulting from evolved moisture can be reduced by baking of the boards before soldering. Under operational circumstances in spaceflight environments, however, this may not be easily accomplished.

4) Porosity arising from entrapped flux can be reduced significantly by implementation of an alternative procedure using a liquid flux that is applied to the joint followed by heating with the soldering iron to activate and evaporate the flux, and subsequent application of a solid solder wire (no flux core).

Table 8 Solder mass added and mean leg-length ratios for combinations of flux type and acceleration level

Test condition	Samples	$1g_e$ avg. mass added, mg	L_T/L_B	Samples	$0g_e$ avg. mass added, mg	L_T/L_B
Flux-core solder	222	25.7 ± 0.8	0.76 ± 0.03	381	26.8 ± 0.8	1.08 ± 0.04
Solid-core solder and liquid flux	91	29.9 ± 1.6	0.71 ± 0.10	198	34.5 ± 1.3	1.16 ± 0.04

5) Visual inspection was shown to be somewhat indicative of joint porosity, but joints made in reduced gravity can pass a visual inspection and still have high levels of internal porosity.

6) The experimental results suggest a very small decrease in heat transfer rate for samples soldered in the $0g_e$ environment compared with those soldered in $1g_e$, but the difference is difficult to distinguish statistically. Conceptually, a small difference would be expected because of the lack of convective cooling by the ambient environment.

7) Solder joints produced in a $0g_e$ environment are more geometrically symmetric than joints produced in a $1g_e$ environment.

8) The quality of manual soldering of plated through-hole configurations is not highly contingent upon operator skill levels. Operators with minimal training and experience can perform comparably to operators with much more extensive experience.

Acknowledgments

This study was part of the Research for Design Program of the National Center for Microgravity Research. This program is funded by NASA's Office of Biological and Physical Research. Additional funding was provided by NASA's International Space Station Program Office. The authors would like to thank the following individuals for their valuable contributions to this project: Gregory Fedor, Jack Kolis, Michael Dobbs, James Withrow, Anthony Butina, Michael Conley, Robert Lowe, William O'Hara, Edward Van Cise, Allison Bahnsen, Owen Farmer, Julio Estrada and the crew of the NASA KC-135 research aircraft. Trade names or manufacturers' names are used in this report for identification only. This usage does not constitute an official endorsement, either expressed or implied, by the National Aeronautics and Space Administration.

References

[1] Carlberg, T., and Liljendahl, M., "Soldering Under Microgravity," *Proceedings of the 4th European Symposium on Materials Sciences under Microgravity*, SP-191, ESA, 1983, pp. 337–342.

[2] Winter, C. A., and Jones, J. C., "The Microgravity Research Experiments (MICREX) Database," NASA TM-108523, Vol. 4, Nov. 1996.

[3] Jones, J. C., and deRooij, A., "Preliminary Investigation of Soldering Electronic Components in Zero-Gravity," *E. W. P. 1554*, ESA, 1989.

[4] Kacpura, T. J., and Acevedo, J. C., "Space Acceleration Measurement System for Free Flyers (SAMS-FF)—Initial Test Results," AIAA Paper 1998-454, Jan. 1998.

[5] Struk, P. M., Pettegrew, R. D., Downs, R. S., and Watson, J. K., "The Effects of an Unsteady Reduced Gravity Environment on the Soldering Process," AIAA Paper 2004-1311; and NASA TM-2004-212946, Jan. 2004.

[6] "Soldered Electrical Connections," NASA STD-8739.3, Dec. 1997.

[7] Pettegrew, R. D., Struk, P. M., Watson, J. K., and Haylett, D. R., "Experimental Methods in Reduced-Gravity Soldering Research," NASA TM-2002-211993, Dec. 2002.

[8] Pettegrew, R. D., Struk, P. M., Watson, J. K., Haylett, D. R., and Downs, R. S., "Gravitational Effects on Solder Joints," *Welding Journal*, Vol. 82, No. 10, Oct. 2003, pp. 44–48.

[9] ASTM Committee E04 on Metallography, "Standard Practice for Determining the Inclusion or Second-Phase Constituent Content of Metals by Automatic Image Analysis," American Society for Testing and Materials Paper E 1245-03, April 2003.

[10] Seah, M. P., Howie, F. H., and Lea, C., "Blowholing in PTH Solder Fillets, Part 3: Moisture and the PCB," *Circuit World*, Vol. 12, No. 4, 1986, pp. 26–33.

[11] Howie, F. H., and Lea, C., "Blowholing in PTH Solder Fillets, Part 2: The Nature, Origin and Evolution of the Gas", *Circuit World*, Vol. 12, No. 4, 1986, pp. 20–25.

[12] Chu, T. Y., "A Hydrostatic Model of Solder Fillets," *Western Electric Engineer*, Vol. 19, No. 2, 1975, pp. 31–42.

[13] Elkouh, A. F., Ramasubramanian, N., Hsu, T. F., Nigro, N. J., Heinrich, S. M., and Lee, P. S., "Prediction of Solder Joint Geometry for an Axisymmetric Through-Hole Joint," *Transactions of the ASME, Journal of Electronic Packaging*, Vol. 119, No. 4, 1997, pp. 268–274.

[14] Heinrich, S. M., "Prediction of Solder Joint Geometry," *Mechanics of Solder Alloy Interconnects*, edited by D. R. Frear, S. N. Burchett, H. S. Morgan, and J. H. Lau, Van Nostrand Reinhold, New York, 1994, Chap. 5, pp. 158–198.

[15] Klein Wassink, R. J., *Soldering in Electronics*, 2nd ed., Electrochemical Publications Ltd., Ayr, Scotland, 1989.

[16] Struk, P. M., Pettegrew, R. D., Downs, R. S., and Watson, J. K., "The Influence of Gravity on Joint Shape for Through-Hole Soldering," AIAA Paper 2005-0541; and NASA TM-2005-213589, Jan. 2005.

L. Peterson
Associate Editor